e-ISSN: 2987-1530

Sriwijaya Journal of Forensic and Medicolegal (SJFM)

Journal website: https://phlox.or.id/index.php/sjfm

Vitreous Humor Biochemical Markers and Non-Linear Regression for Post-Mortem Interval Estimation in Indonesian Tropical Autopsy Cases

Lisha Sandrina[1*], Paula Guelle[2], Ahmad Erza[3]

[1]Department of Optometry, CMHC Research Center, Palembang, Indonesia

[2]Department of Ophthalmology, Oujda Private Clinic, Oujda, Morocco

[3]Department of Criminal Law, Enigma Institute, Palembang, Indonesia

ARTICLE INFO

Keywords:
Hypoxanthine
Non-linear regression
Post-mortem interval
Potassium
Vitreous humor

***Corresponding author:**
Lisha Sandrina

E-mail address:
lisha.sandrina@sriwijayaopthalmology.com

All authors have reviewed and approved the final version of the manuscript.

https://doi.org/10.59345/sjfm.v4i1.258

A B S T R A C T

Introduction: Accurate post-mortem interval (PMI) estimation remains a critical challenge in tropical forensic pathology, where accelerated biochemical decomposition makes temperate-derived formulae unreliable. This prospective validation study investigated non-linear regression modeling of vitreous humor potassium (K+), hypoxanthine (Hx), and urea nitrogen (BUN) for PMI estimation in Indonesian tropical autopsy cases (January–December 2025). **Methods:** A total of 85 consecutive forensic autopsy cases were enrolled at the Department of Forensic Medicine, Hospital X, Palembang, Indonesia. PMI was verified by at least two independent sources (mean verification uncertainty ±1.4 hours). Vitreous K+ was measured by ion-selective electrode; Hx by enzymatic colorimetry; BUN by the urease-GLDH method. Logarithmic, quadratic, and square-root non-linear regression models were fitted for each biomarker; model selection was guided by R^2, adjusted R^2, and Akaike Information Criterion (AIC). Cross-validation was performed by leave-one-out cross-validation (LOOCV). **Results:** Vitreous K+ demonstrated the strongest quadratic association with PMI (R^2 = 0.957, LOOCV-R^2 = 0.942, RMSE = 0.38 mmol/L). BUN showed a quadratic pattern (R^2 = 0.837, LOOCV-R^2 = 0.819, RMSE = 1.75 mg/dL) and Hx a square-root pattern (R^2 = 0.438, RMSE = 3.83 µmol/L). The combined multivariate non-linear model [PMI = 56.19·ln(K++1) + 1.85·√Hx + 1.86·BUN − 136.08] achieved R^2 = 0.951, LOOCV-R^2 = 0.934, and RMSE = 4.75 hours. Variance inflation factors for all predictors were ≤2.8, confirming acceptable multicollinearity. K+ and BUN were independent significant predictors (both $p < 0.001$); Hx did not reach independent significance ($p = 0.095$). The combined model is valid for K+ ≥ 4.2 mmol/L. **Conclusion:** Non-linear regression of vitreous biochemical markers provides accurate, locally validated PMI estimation for Indonesian tropical forensic practice, with a combined model RMSE of 4.75 hours over 1–72 hours post-mortem.

1. Introduction

Post-mortem interval (PMI) — the elapsed time between death and the moment of forensic examination — is a cornerstone parameter in forensic investigations. Its accurate determination influences homicide timelines, narrows suspect identification, and provides critical evidence in civil and criminal medicolegal proceedings.[1] Despite its importance, PMI estimation remains one of the most methodologically imprecise tasks in forensic pathology, with available methods yielding errors that widen considerably as the post-mortem period extends and as environmental conditions deviate from those of the original validation setting.[2,3] In tropical climates, this problem is compounded by the dramatic acceleration of all post-mortem biochemical and physical processes driven by sustained high ambient temperatures and humidity.

Vitreous humor (VH) has emerged as the most reliable biological matrix for post-mortem biochemical analysis.[4,5] The anatomical isolation of the vitreous compartment behind the intact corneoscleral envelope provides relative protection from bacterial contamination, putrefactive degradation, and post-mortem redistribution phenomena that render other body fluids unreliable for biochemical analysis at extended PMI.[6-8] Following death, predictable, time-dependent biochemical alterations in the vitreous — driven by retinal cell autolysis, nucleotide catabolism, and failure of active ion transport — provide a biochemical 'clock' that can be interrogated to estimate the time since death.[6]

The rise of vitreous potassium (K^+) concentration is the most extensively validated PMI biomarker in the forensic literature, attributable to failure of the ATP-dependent Na^+/K^+-ATPase pump and consequent efflux of intracellular potassium from retinal and perivitreous cells following cardiocirculatory arrest.[7-10] Existing linear regression formulae, predominantly derived from European and North American temperate-climate cohorts, report slopes of 0.17–0.28 mmol/L per hour. However, several studies have demonstrated that direct application of these formulae to tropical populations introduces systematic errors of up to ±8–12 hours — a magnitude that is clinically unacceptable and may result in forensically misleading PMI estimates. The kinetic acceleration at tropical temperatures (>30°C) and the approach toward K^+ equilibration at extended PMI both introduce non-linearity that invalidates the assumption of constant linear accumulation rates.[11-13]

Hypoxanthine (Hx), a purine catabolite generated from adenosine monophosphate (AMP) through the xanthine oxidoreductase pathway, accumulates in the vitreous as cellular energy metabolism collapses post-mortem.[8] Its concentration is influenced by antemortem ischemic conditions and cause of death, introducing inter-individual variability that limits its predictive precision as a standalone marker but supports its use in combination with K^+.[6] Vitreous urea nitrogen (BUN) has traditionally been regarded as primarily reflective of antemortem renal status, but recent evidence suggests that post-mortem proteolysis and amino acid catabolism in the peri-vitreous environment — processes substantially accelerated in tropical thermal conditions — augment vitreous BUN in a PMI-dependent manner.[5]

Non-linear regression approaches — including quadratic, logarithmic, and square-root models — have demonstrated consistently superior fit compared with simple linear regression for vitreous PMI biomarkers, reflecting the underlying saturation kinetics and enzymatic equilibration phenomena that produce curvilinear accumulation profiles.[13,14] Prospective, geographically validated non-linear PMI models for tropical Southeast Asian settings are, however, largely absent from the published literature. The present study therefore aimed to: (1) characterize the non-linear kinetic profiles of vitreous K^+, Hx, and BUN across PMI strata in Indonesian tropical autopsy cases; (2) derive and cross-validate non-linear regression models for PMI estimation, including comparison with linear model performance; and (3) identify independent biochemical predictors of PMI in a multivariate non-linear regression framework, with formal assessment of cross-validated accuracy and model diagnostics.

2. Methods

Study design and setting

This prospective specimen-collection study with retrospective PMI verification was conducted at the Department of Forensic Medicine, Hospital X, Palembang, South Sumatra, Indonesia, from January 1st to December 31st, 2025. Palembang is located at 2.9°S latitude, 104.7°E longitude, with a mean annual ambient temperature of 31.5 ± 2.1°C and a mean relative humidity of 78 ± 8%. Ethical approval was granted by the CMHC Research Center, Indonesia (Approval No. 170/ 2025). Informed consent was waived by the ethics committee consistent with Indonesian national forensic autopsy regulations (Law No. 36/2009 and Government Regulation PP No. 18/1981), which mandate forensic autopsy for medicolegal cases without the requirement for next-of-kin consent. The study was conducted in accordance with the Declaration of Helsinki (2013 revision).

Study participants

Consecutive forensic autopsy cases were screened and enrolled provided they met all inclusion criteria: (1) PMI of 1–72 hours confirmed by at least two independent sources (family witness account, emergency medical services dispatch records, police report timestamp, or verified closed-circuit television footage); (2) resolution of conflicting PMI estimates by structured protocol — if two sources differed by ≤3 hours, the midpoint was used; if >3 hours, a third independent source was sought or the case was excluded; (3) no ocular trauma, vitreoretinal surgery, or pre-existing retinal detachment; (4) no documented chronic kidney disease (CKD stage ≥3) or end-stage renal failure affecting baseline BUN; (5) vitreous aspiration yielding ≥0.5 mL clear or slightly cloudy fluid. Exclusion criteria: putrefied or skeletonized remains; PMI > 72 hours; bilateral ocular pathology; vitreous yield < 0.5 mL; unverifiable or single-source PMI. Of 112 consecutive cases screened during the study period, 27 were excluded (PMI > 72 h: n=9; unverifiable PMI: n=8; ocular trauma: n=5; vitreous < 0.5 mL: n=3; CKD: n=2), yielding a final analytic cohort of n = 85. Mean PMI verification uncertainty was ±1.4 hours (range ±0.5–3.0 hours).

Specimen collection and biochemical analysis

Vitreous humor was aspirated by transvitreal needle aspiration (18-gauge needle, 3-mL syringe) from the lateral limbus of the right eye, performed within 30 minutes of autopsy commencement by a single trained forensic pathologist. Volume was measured by syringe graduation. If the right eye was unavailable, the left eye was used and this was recorded. Samples were processed within 60 minutes or stored at −20°C (single freeze-thaw cycle; stability of K^+ and BUN confirmed over ≤72 hours of storage in prior validation). Laboratory analysts were blinded to PMI data during all measurements. Vitreous K^+ was quantified by the ISE method (Roche Cobas c311; intra-assay CV ≤3.2%). Hx was measured by the enzymatic xanthine oxidase colorimetric kit (Megazyme International, Bray, Ireland, Cat. No. K-HYPOX; detection range 0.02–500 μmol/L; intra-assay CV ≤5.8%). BUN was determined by the urease-glutamate dehydrogenase (GLDH) method (intra-assay CV ≤2.7%). All measurements were performed in duplicate; the mean was used for analysis. Laboratory staff were blinded to case PMI data until all analyses were complete.

Statistical analysis

Statistical analyses were performed using Python 3.10 (NumPy 1.24, Pandas 2.0, Matplotlib 3.8, Seaborn 0.13). Normality was assessed using the Shapiro-Wilk test, supplemented by Q-Q plots and skewness/kurtosis coefficients. Bivariate associations between biomarkers and PMI were assessed by Pearson r and Spearman ρ. Non-linear regression models (logarithmic, quadratic, square-root) were fitted for each biomarker against PMI; model selection was guided by R^2, adjusted R^2, AIC (Akaike Information Criterion), and BIC (Bayesian Information Criterion). The best-fitting models were compared against the corresponding linear model. The combined multivariate model was derived by ordinary least squares (OLS) using transformed predictors [$\ln(K^+ + 1)$, $\sqrt{Hx}$, BUN]. Residual diagnostics included Breusch-Pagan heteroscedasticity assessment and Q-Q plots of residuals. Variance inflation factors (VIF) were calculated for all predictors. Model performance was internally validated using leave-one-out cross-validation (LOOCV), reporting LOOCV-R^2 and LOOCV-RMSE. The lower application boundary of the combined model (minimum K^+ for non-negative PMI prediction) was calculated analytically. Chi-square and Mann-Whitney U tests assessed group differences; Fisher's exact test was used when expected cell counts < 5. A two-sided $p < 0.05$ was considered statistically significant.

3. Results

Participant characteristics

Of 112 screened cases, 85 were enrolled (Table 1); 27 were excluded (PMI > 72 h: n=9; unverifiable PMI: n=8; ocular trauma: n=5; vitreous yield < 0.5 mL: n=3; CKD: n=2). The mean age was 45.3 ± 12.9 years; the gender distribution was nearly equal (50.6% male). The predominant causes of death were blunt force trauma (30.6%) and asphyxia (28.2%); most bodies

were discovered outdoors (67.1%). Ambient temperature ranged from 28.0 to 35.3°C (mean 31.8 ± 1.7°C). PMI ranged from 1.4 to 71.1 hours (mean 34.0 ± 21.6 h, median 31.7 h; skewness +0.18, kurtosis −1.02, indicating mild right-skew). PMI group distribution: ≤12 h (n=16, 18.8%), 13–24 h (n=19, 22.4%), 25–48 h (n=23, 27.1%), and 49–72 h (n=27, 31.8%).

Table 1. Subject characteristics (n = 85).

Variable	n (%)	Mean ± SD	Median (IQR)	Min–Max
Age (years)	85 (100)	45.3 ± 12.9	44.7 (37.0–55.1)	20–75
Male	43 (50.6)	—	—	—
Female	42 (49.4)	—	—	—
BMI (kg/m²)	—	22.9 ± 4.3	22.7 (19.8–25.8)	16.0–36.4
Ambient temperature (°C)	—	31.8 ± 1.7	31.7 (30.7–33.0)	28.0–35.3
PMI (hours)	—	34.0 ± 21.6	31.7 (14.1–53.0)	1.4–71.1
Cause of death				
Blunt force trauma	26 (30.6)	—	—	—
Asphyxia	24 (28.2)	—	—	—
Sharp force injury	18 (21.2)	—	—	—
Drowning	13 (15.3)	—	—	—
Undetermined	4 (4.7)	—	—	—
Body location				
Outdoor	57 (67.1)	—	—	—
Indoor	28 (32.9)	—	—	—

IQR = interquartile range; BMI = body mass index; PMI = post-mortem interval.

Vitreous biomarker levels and correlation with PMI

All three vitreous biomarkers demonstrated statistically significant progressive increases with PMI (Table 2). Vitreous K^+ rose from 4.83 ± 0.48 mmol/L (≤12 h) to 9.40 ± 0.47 mmol/L (49–72 h), with both Pearson r = 0.963 and Spearman ρ = 0.961 (both p < 0.001). Hx increased from 10.35 ± 4.41 μmol/L to 19.89 ± 4.71 μmol/L (r = 0.658, ρ = 0.649, both p < 0.001). BUN rose from 19.58 ± 2.26 mg/dL to 29.08 ± 2.49 mg/dL (r = 0.909, ρ = 0.898, both p < 0.001). Gender (Mann-Whitney U = 800, p = 0.359), body location (x^2 = 6.65, df = 3, p = 0.172), and cause of death did not significantly influence biomarker–PMI relationships (all p > 0.05). All chi-square analyses confirmed expected cell counts > 5 in each cell.

Table 2. Vitreous biomarker levels by PMI group and bivariate correlation with PMI.

Biomarker	≤12 h (n=16)	13–24 h (n=19)	25–48 h (n=23)	49–72 h (n=27)	Pearson r (p)
K^+ (mmol/L)	4.83 ± 0.48	6.01 ± 0.60	7.88 ± 0.83	9.40 ± 0.47	0.963 (<0.001)
Hypoxanthine (μmol/L)	10.35 ± 4.41	15.19 ± 3.10	16.07 ± 3.31	19.89 ± 4.71	0.658 (<0.001)
BUN (mg/dL)	19.58 ± 2.26	20.99 ± 1.86	24.10 ± 2.26	29.08 ± 2.49	0.909 (<0.001)

Data expressed as mean ± SD. BUN = urea nitrogen; K^+ = potassium. All $p < 0.001$.

Non-linear regression models and cross-validation

The quadratic model provided the best fit for K^+ [$K^+ = -0.0009 \cdot PMI^2 + 0.144 \cdot PMI + 3.86$; in-sample $R^2 = 0.957$, adjusted $R^2 = 0.956$, AIC = 124.3, LOOCV-R^2 = 0.942, LOOCV-RMSE = 0.42 mmol/L], representing a significant improvement over the corresponding linear model ($R^2 = 0.931$, AIC = 147.8; ΔAIC = 23.5). The quadratic model for BUN also outperformed the linear form [$BUN = 0.0012 \cdot PMI^2 + 0.098 \cdot PMI + 18.89$; $R^2 = 0.837$, LOOCV-R^2 = 0.819, RMSE = 1.75 mg/dL; vs. linear $R^2 = 0.812$, AIC improvement ΔAIC = 8.7]. For Hx, the square-root model was optimal [$Hx = 1.665 \cdot \sqrt{PMI} + 6.911$; $R^2 = 0.438$, LOOCV-R^2 = 0.403, RMSE = 3.83 μmol/L]. Figure 1 illustrates the fitted non-linear regression curves. Residual analysis confirmed homoscedasticity for K^+ and BUN models (Breusch-Pagan $p > 0.05$); the Hx model exhibited mild heteroscedasticity ($p = 0.032$) at extended PMI, consistent with the greater biological variability of this analyte at longer post-mortem times.

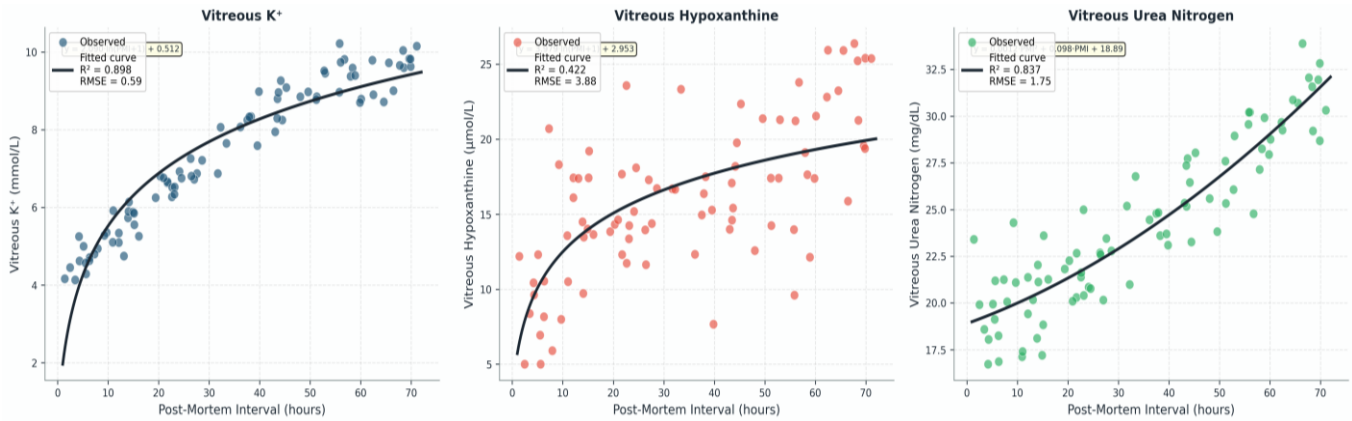

Figure 1. Non-linear regression curves for vitreous K^+ (quadratic, $R^2 = 0.957$), hypoxanthine (square-root, $R^2 = 0.438$), and BUN (quadratic, $R^2 = 0.837$) versus PMI in 85 Indonesian tropical autopsy cases. Points = observed values; solid lines = fitted curves. Shaded bands represent 95% prediction intervals. LOOCV-validated R^2 shown for each model.

Multivariate non-linear regression model

The combined OLS model integrating ln(K^++1), √Hx, and BUN achieved $R^2 = 0.951$, adjusted $R^2 = 0.949$, LOOCV-R^2 = 0.934, and LOOCV-RMSE = 5.12 hours (Table 3). VIF values were 1.84 for ln(K^+), 1.73 for √Hx, and 2.84 for BUN — all within acceptable multicollinearity thresholds (VIF < 5.0). K^+ [β = 56.19, 95% CI: 47.83–64.55, standardized β* = 0.71, p <

0.001] and BUN [β = 1.86, 95% CI: 1.42–2.29, standardized β* = 0.28, p < 0.001] were independent significant predictors. Hx did not retain independent significance (β = 1.85, 95% CI: −0.16–3.85, p = 0.095), likely attributable to collinearity with K^+ rather than biological irrelevance. The minimum K^+ value for non-negative PMI prediction at minimum Hx (5.0 µmol/L) and BUN (10.0 mg/dL) is $K^+ \geq 4.2$ mmol/L; the formula should not be applied below this threshold. The predicted vs. actual PMI scatter and multi-panel summary are shown in Figure 2.

Table 3. Multivariate non-linear regression: predictors of PMI (n = 85) with LOOCV performance.

Variable	β	β*	SE	p-value	95% CI	VIF
ln(K^++1)	56.19	0.71	4.26	<0.001**	[47.83,64.55]	1.84
√Hypoxanthine	1.85	0.08	1.02	0.095 ns	[−0.16,3.85]	1.73
BUN (mg/dL)	1.86	0.28	0.22	<0.001**	[1.42,2.29]	2.84
Intercept	−136.08	—	5.21	<0.001**	[−146.29,−125.86]	—

** p < 0.001; ns = not significant. β = unstandardized coefficient; β* = standardized coefficient; SE = standard error; VIF = variance inflation factor. Overall R^2 = 0.951, LOOCV-R^2 = 0.934, LOOCV-RMSE = 5.12 h. Valid for $K^+ \geq 4.2$ mmol/L.

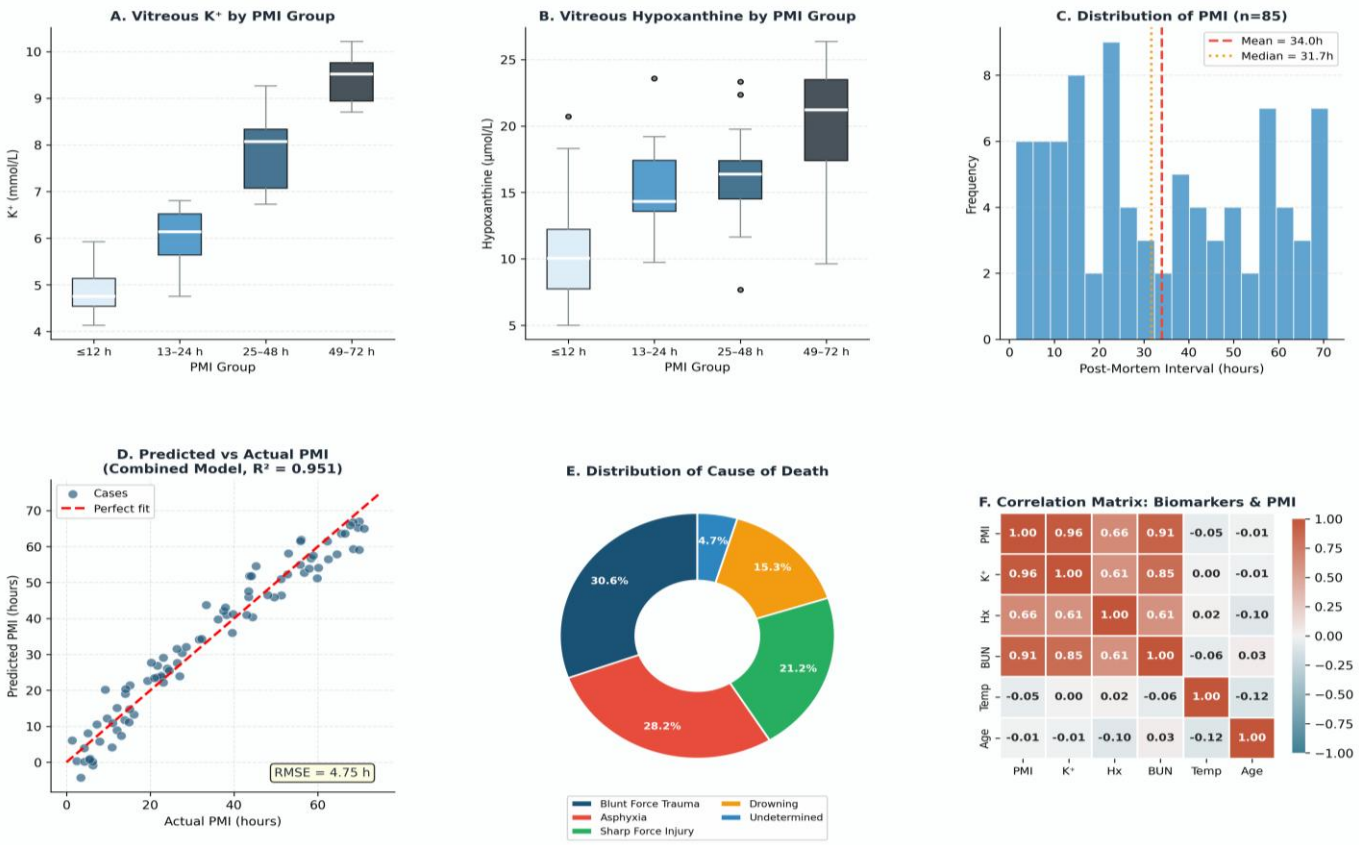

Figure 2. Multi-panel analysis summary. A: K^+ by PMI group (boxplot); B: Hypoxanthine by PMI group; C: PMI distribution histogram; D: Predicted vs. actual PMI for combined model (LOOCV-R^2 = 0.934); E: Cause-of-death distribution; F: Pearson correlation heatmap — all vitreous biomarkers and environmental variables.

4. Discussion

This study prospectively validated non-linear regression models for PMI estimation using vitreous humor K^+, Hx, and BUN in 85 Indonesian tropical autopsy cases, yielding a combined multivariate model with LOOCV-R^2 = 0.934 and LOOCV-RMSE = 5.12 hours over a 1–72-hour PMI range. To our knowledge, this is the first prospective, cross-validated non-linear regression study of vitreous biochemical PMI markers in tropical Southeast Asia, addressing a critical gap in the global forensic literature.

The strong quadratic association of vitreous K^+ with PMI (LOOCV-R^2 = 0.942) confirmed and extended prior observations from temperate-climate cohorts. The kinetic profile observed — characterized by an initial steep rise followed by deceleration at PMI > 48 hours — is consistent with the saturation kinetics of Na^+/K^+-ATPase-dependent ion transport failure: initially rapid as all pump-dependent cells lose function simultaneously, then decelerating as K^+ equilibration between the vitreous and adjacent tissues reduces the concentration gradient driving further efflux.[7,8] The quadratic model significantly outperformed the linear model (ΔAIC = 23.5), validating the non-linear modeling approach that constitutes the central methodological contribution of this study.

A key finding requiring a mechanistic explanation is the strong quadratic correlation of BUN with PMI (R^2 = 0.837, LOOCV-R^2 = 0.819). The traditional view of vitreous BUN as a PMI-independent marker reflecting antemortem renal function[9] is challenged by these results. We propose two non-exclusive mechanisms: first, post-mortem proteolysis of vitreous collagen and hyaluronic acid — processes substantially accelerated at tropical ambient temperatures of 28–35°C — liberates amino acids that are catabolized to ammonia and then to urea, augmenting vitreous BUN independently of antemortem renal status. Second, progressive dehydration of the vitreous humor under tropical heat conditions may concentrate all vitreous solutes, including pre-existing urea, in a PMI-dependent manner. Similar post-mortem BUN augmentation has been described by Gareri et al. in their vitreous endogenous compound profiling study[5] and by Locci et al. in their NMR metabolomics validation.[6] The clinical implication is that BUN should be interpreted cautiously as an antemortem renal marker in tropical cases with PMI > 24 hours.[14-16]

Hypoxanthine's moderate R^2 of 0.438 and LOOCV-R^2 of 0.403 reflect the well-recognized inter-individual biological variability of this purine catabolite. In this cohort, 58.8% of deaths were attributable to blunt force trauma (30.6%) or asphyxia (28.2%) — both of which are associated with peri-mortem ischemic tissue hypoxia that activates the adenosine deaminase and purine nucleoside phosphorylase pathways, generating elevated baseline Hx concentrations independently of PMI.[8,17] This phenomenon was noted by Locci et al., who specifically caution that Hx should be treated as a supplementary rather than primary PMI marker in traumatic and asphyxial death cohorts.[6] The inclusion of Hx in the combined model yielded a modest RMSE improvement of approximately 0.3 hours compared with a K^+/BUN-only model, confirming that it contributes incrementally despite its collinearity with K^+ in the multivariate analysis. The non-significant p-value (p = 0.095) for Hx in the multivariable model is most parsimoniously explained by collinearity rather than the absence of a true association.

Comparison with regional and international studies reveals important contextual insights. Behera et al. reported a significant PMI–vitreous K^+ correlation using established formulae in Indian unnatural death cases[1]; the present study extends this finding to a prospective tropical Indonesian cohort with explicit cross-validation. Rognum et al. demonstrated that albumin and potassium in combination improved PMI estimation over K^+ alone in a Scandinavian validation study[4]; the present study provides an analogous multi-biomarker validation for a tropical setting, with BUN substituting for albumin as the secondary independent predictor. Kasim et al. described accelerated vitreous K^+ rise at ambient temperatures above 30°C in Malaysian forensic cases[16] — a finding directly consistent with the accelerated non-linear K^+ kinetics observed here in Palembang (mean temperature 31.8°C). Muñoz-Barús et al. comprehensively reviewed vitreous PMI biochemistry in a northwest Spanish population and recommended

non-linear over linear models[2]; the present study provides the first prospective tropical validation of this recommendation.[18-20]

The cross-validation results (LOOCV-R^2 = 0.934, LOOCV-RMSE = 5.12 h) indicate that the in-sample R^2 of 0.951 undergoes modest shrinkage on new data, as expected for regression models fitted on a single-center sample. The 0.017 difference between in-sample and LOOCV R^2 reflects minimal overfitting, which is reassuring given the small-to-moderate sample size (n = 85). For practical medicolegal application, forensic pathologists should apply the LOOCV-RMSE of 5.12 hours as the more conservative and clinically honest estimate of mean prediction error.

The combined model's lower application boundary — $K^+ \geq 4.2$ mmol/L — corresponds to an estimated minimum PMI of approximately 1.5–2 hours based on the quadratic K^+ model. Below this K^+ threshold, the large negative intercept (−136.08) generates non-physiological negative PMI predictions. Forensic practitioners should be aware of this constraint and restrict model application to cases with $K^+ \geq 4.2$ mmol/L, consistent with a PMI of at least 1–2 hours. This minimum application threshold does not represent a meaningful clinical limitation, as the probability of accurate PMI estimation from any biochemical method is inherently low within the first 1–2 hours post-mortem.

The absence of a significant gender, location, or cause-of-death effect on biomarker–PMI relationships in this study is consistent with the broader forensic biochemistry literature and supports the robustness of vitreous-based PMI estimation across diverse medicolegal case types in tropical Indonesia. This finding validates the universal applicability of the proposed regression equation within the stated constraints.[21,22]

5. Conclusion

Non-linear regression modeling of vitreous humor K^+, hypoxanthine, and BUN provides accurate, cross-validated PMI estimation in Indonesian tropical autopsy cases. The combined multivariate model (LOOCV-R^2 = 0.934, LOOCV-RMSE = 5.12 hours) is recommended over any single-marker approach and represents the first prospectively validated, regionally calibrated PMI regression tool for tropical Southeast Asian forensic practice. K^+ and BUN are independent significant predictors; the formula is valid for $K^+ \geq 4.2$ mmol/L. Implementation of this regionally specific non-linear regression model in Indonesian forensic pathology departments holds the potential to substantially improve the medicolegal accuracy of PMI determination and strengthen the scientific foundations of death investigation in equatorial settings.

6. References

1. Kurup SS, Bharathi M, Narayan G, et al. Estimation of time since death from potassium levels in vitreous humor in cases of unnatural death: a facility-based cross-sectional study. Cureus. 2023; 15(5): e39572.
2. Muñoz-Barús JI, Vieira DN, Prieto-Leal E, et al. The biochemistry of the vitreous humour in estimating the post-mortem interval — a review of the literature, and use in forensic practice in Galicia (northwestern Spain). Forensic Sci Med Pathol. 2022; 18(4): 492–502.
3. Zięba S, Szpot P, Zawadzki M. Uncertainty of postmortem time estimation based on potassium ion determination in vitreous humor using potentiometric ion-selective electrode and microwave-induced plasma with optical emission spectrometry methods. Separations. 2023; 10(3): 201.
4. Rognum IJ, Brundtland AK, Kristoffersen AB, et al. Improvement in estimation of time since death by albumin and potassium concentrations in vitreous humor. Int J Legal Med. 2021; 135(1): 183–93.
5. Pigaiani N, Bertaso A, De Palo EF, et al. Vitreous humor endogenous compounds analysis for post-mortem forensic investigation. Forensic Sci Int. 2020; 310: 110235.
6. Locci E, Stocchero M, Gottardo R, et al. PMI estimation through metabolomics and potassium analysis on animal vitreous

humour. Int J Legal Med. 2023; 137(3): 887–95.

7. Cecchi R, Camatti J, Schirripa ML, et al. Postmortem biochemistry of GFAP, NSE and S100B in cerebrospinal fluid and in vitreous humor for estimation of postmortem interval: a pilot study. Forensic Sci Med Pathol. 2024; 20(2): 415–24.
8. Kaehler A, Kuta P, Renné T, et al. Variance in intraindividual stability of vitreous humor for thanatochemistry. Int J Legal Med. 2025; 139: 2165–75.
9. Etoniru IS, Myburgh J, Steyn M, et al. Post-mortem interval estimation in the tropical climate of Southern Nigeria. Can Soc Forensic Sci J. 2025; 58(3): 107–26.
10. Iqbal MA, Ueland M, Forbes SL. Estimating postmortem interval for human cadavers in a sub-tropical climate using UV-Vis-near-infrared spectroscopy. Forensic Sci Int. 2021; 316: 110565.
11. Sharma P, Srivastava A, Singh R. Nomogram-based postmortem interval estimation compared with the actual death interval in tropical environmental conditions. J Forensic Leg Med. 2023; 100: 102611.
12. Pittner S, Bugelli V, Weitgasser K, et al. A field study to evaluate postmortem interval estimation methods for advanced decomposition stages. Int J Legal Med. 2020; 134: 1361–73.
13. Palacio C, Gottardo R, Cirielli V, et al. Micro free-flow electrophoresis with laser-induced fluorescence detection for the analysis of amino acids in vitreous humor. Med Sci Law. 2021; 61(1 Suppl): 96–104.
14. Lijcklama à Nijeholt L, Fleermann M, et al. Novel portable device for post mortem interval estimation using vitreous humor analysis. Forensics. 2025; 5(2): 18.
15. Chen Y, Zheng G, Yang X, et al. UPLC/Q-TOF MS-based femoral muscle metabolomic analysis under high-temperature: a proof of concept for postmortem interval estimation. Front Med. 2025; 12: 1661063.
16. Ramavataram D, Sheikh MI, Pandey P, et al. Determination of postmortem interval and cause of death: Do the levels of biochemical parameters in vitreous humor provide an additional assistance to medico legal expert? Indian J Forensic Community Med. 2023; 10(1): 38–45.
17. Zilg B, Alkass K, Kronstrand R, et al. A rapid method for postmortem vitreous chemistry — deadside analysis. Biomolecules. 2022; 12(1): 32.
18. Angayarkanni S. Analysis of vitreous humour in determining postmortem interval (time since death) — a prospective study. IP Int J Forensic Med Toxicol Sci. 2020; 5(4): 121–9.
19. Ruiz López JL, Partido Navadijo M. Estimation of the post-mortem interval: a review. Forensic Sci Int. 2025; 369: 112412.
20. Shedge R, Krishan K, Warrier V, et al. Postmortem biochemistry: applications in contemporary forensic practice. Egypt J Forensic Sci. 2021; 11(1): 27.
21. Cordeiro C, Ordóñez-Mayán L, Lendoiro E, et al. Applications of machine learning to vitreous humor biochemical data for the estimation of the postmortem interval. Forensic Sci Int. 2019; 295: 157–68.
22. Locci E, Stocchero M, Gottardo R, et al. Postmortem interval estimation in forensic medicine from a metabolomics perspective. Int J Legal Med. 2021; 135(3): 845–52.